



Polar of a 2D Glider Airfoil. Optimization and roughness effects

Computational Fluid Dynamics

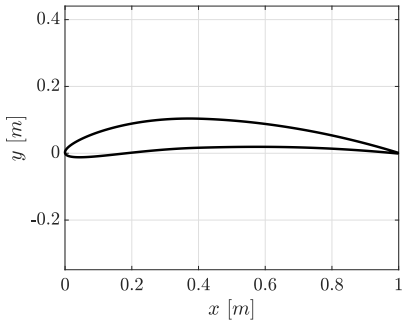
M. Mady, F. Libretti, A. Strambaci, J. Monmeneu, N. Couto

- ① Problem geometry and setup
- ② Mesh convergence
- ③ Polar
- ④ Law of the Wall
- ⑤ Optimization
- ⑥ Roughness

- 1 Problem geometry and setup
- 2 Mesh convergence
- 3 Polar

- 4 Law of the Wall
- 5 Optimization
- 6 Roughness

The airfoil considered for the analysis is a NACA 6409, which has a chord equal to 1 m. The computational domain consists on a circle centered in the origin of the coordinate system, which coincides to the leading edge of the airfoil.



The freestream properties have been selected in order to match the experimental data available for the NACA 6409 airfoil. Two different cases are taken into account.

Velocity [m/s]	Density [kg/m ³]	Reynolds Number	Mach Number
0.9288	1.225	61400	0.0027
3.0722	1.225	203100	0.009

Air flow is assumed to be incompressible due to the low Mach number; therefore the *INC_RANS* solver is used for all simulations.

- ① Problem geometry and setup
- ② Mesh convergence
- ③ Polar

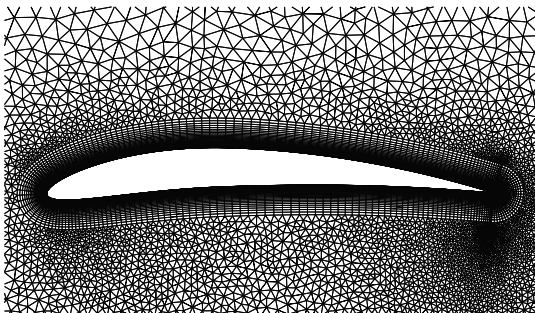
- ④ Law of the Wall
- ⑤ Optimization
- ⑥ Roughness

The value for the Venkatakrishnan slope limiter ϵ coefficient was obtained following:

$$\epsilon^2 = K_{SU2}^3$$

where K_{SU2} is the threshold parameter. $K_{SU2,2}$ was computed starting from a guess value of $K_{SU2,1} = 0.1$ corresponding to the finest grid and then corrected according to the average cell size of the different grids studied following:

$$\frac{K_{SU2,1}}{K_{SU2,2}} = \frac{\bar{\Delta}_1}{\bar{\Delta}_2}$$



Thickness	0.07 <i>m</i>
First cell size	0.00001 <i>m</i>
Ratio	1.1
Fan number of elements	30

The analysis concerning the farfield is divided in two blocks:

- Ratio between farfield radius and farfield element size
- Farfield radius selection

Farfield size [m]	Number of Elements
15	51239
30	93439
45	150485
60	226341

Farfield size [m]	H [m]
15	0.5
30	1
60	2
120	4
240	8

Once the farfield is set, the generation of three different grids, with an increasing refinement level, is carried out according to the grid convergence index procedure.

\bar{h} [m]	r_{ji}	H [m]	Number of Elements
1.0809	/	5.33	38247
0.8189	1.32	4	66876
0.6160	1.32	2	120537

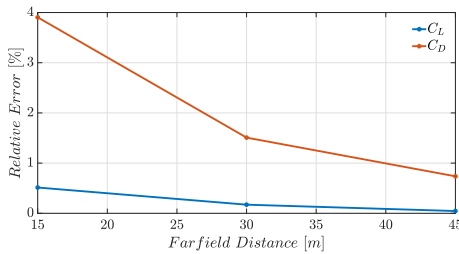
The grid convergence index (GCI) is an equivalent error due to discretization, expressed as a percentage, which is associated to the upper and lower bound on the deviation of a numerical results with respect to the exact solution, as a consequence of the problem discretization.

$$GCI_{21} = FS \frac{e_a^{21}}{r_{21}^p - 1}$$

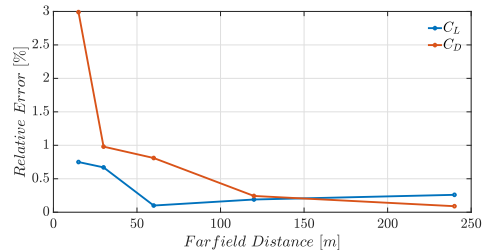
- e_a^{21} - relative error between grid 2 and grid 1
- r_{21} - refinement factor between grid 2 and grid 1
- p - apparent order of convergence
- FS - safety factor

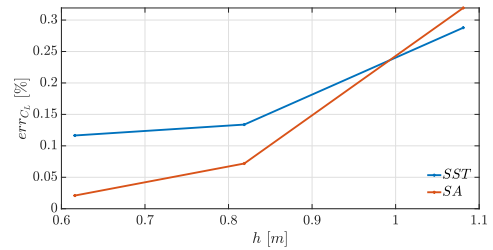
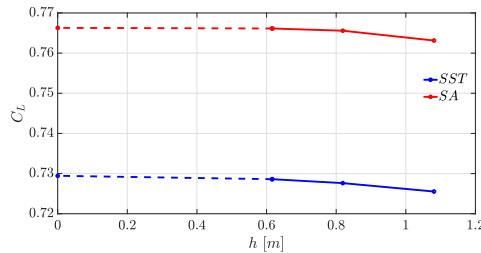
Farfield assessment results

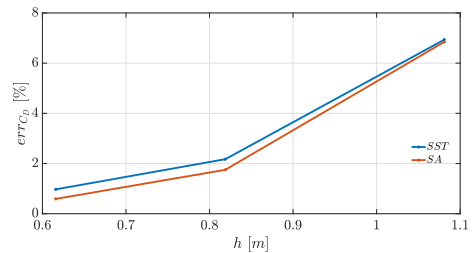
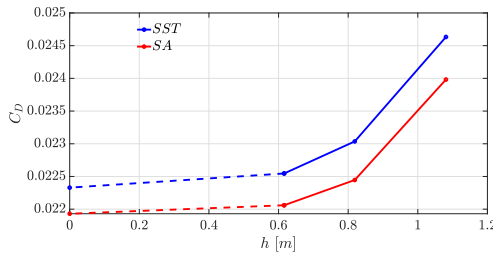
- Ratio between farfield radius and farfield element size

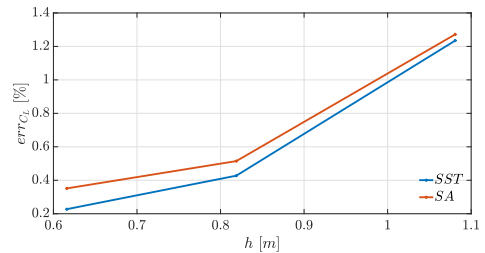
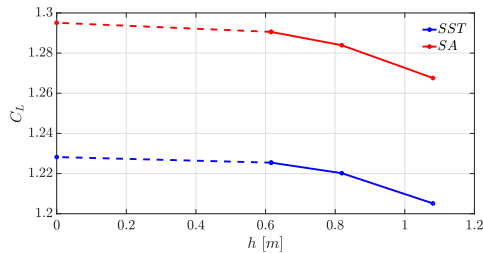


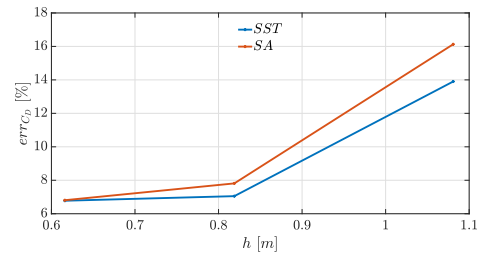
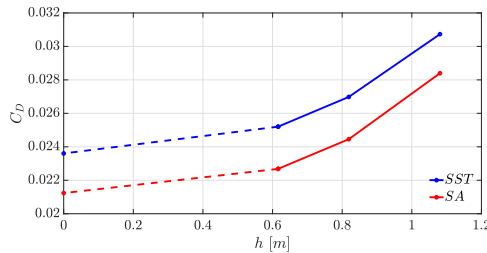
- Farfield radius selection











Grid convergence index results

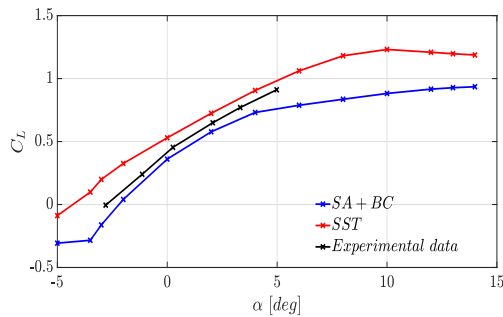
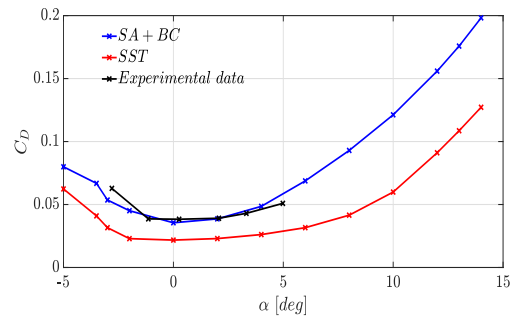
Grid	GCI_{C_L} [%] SA	GCI_{C_D} [%] SA	GCI_{C_L} [%] SST	GCI_{C_D} [%] SST
Fine	0.0262	0.734	0.15	1.2
Medium	0.11	2.72	0.3	3.69

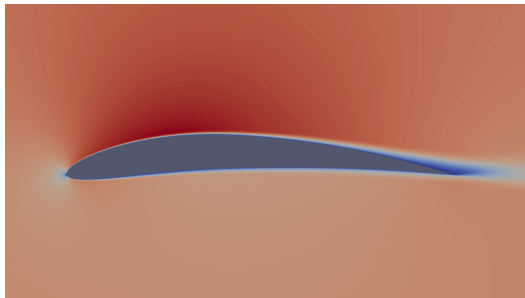
GCI analysis, $\alpha = 2^\circ$, $Re = 61400$

Grid	GCI_{C_L} [%] SA	GCI_{C_D} [%] SA	GCI_{C_L} [%] SST	GCI_{C_D} [%] SST
Fine	0.44	7.97	0.28	7.93
Medium	1.03	17.02	0.78	16.12

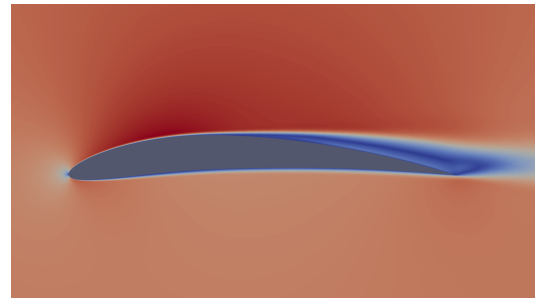
GCI analysis, $\alpha = 6.94^\circ$, $Re = 203100$

- ① Problem geometry and setup
- ② Mesh convergence
- ③ Polar
- ④ Law of the Wall
- ⑤ Optimization
- ⑥ Roughness

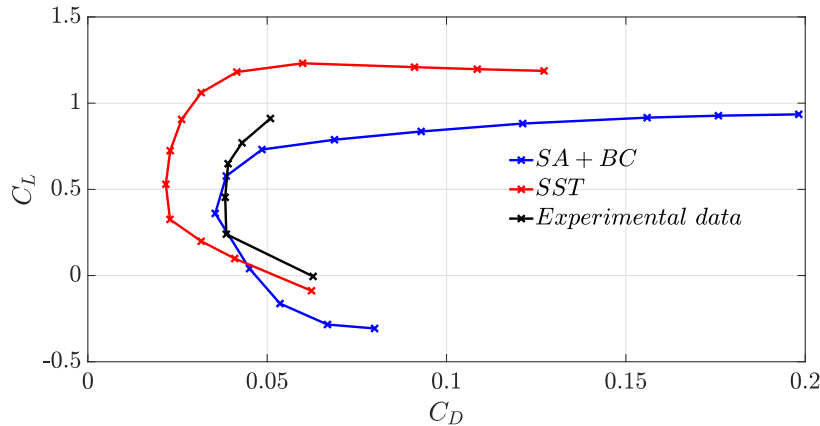
(a) C_L vs α (b) C_D vs α

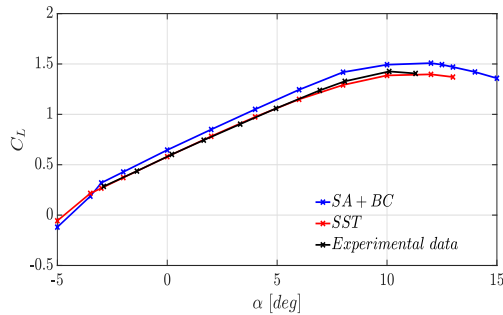
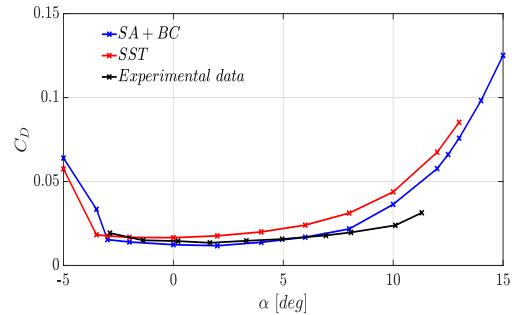


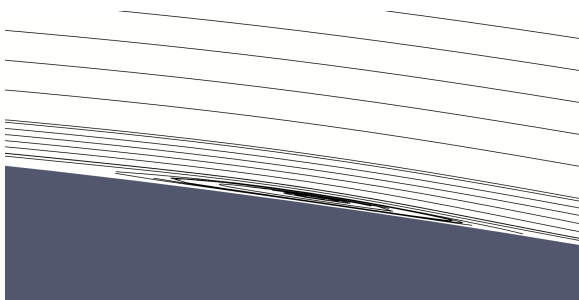
(a) *SST Velocity contours*



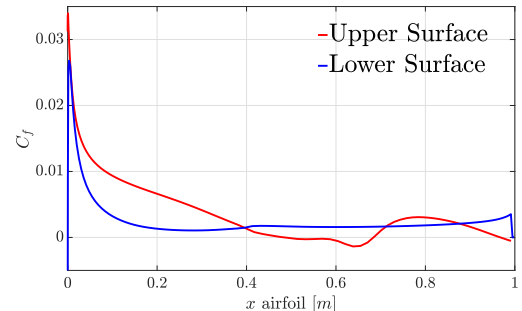
(b) *SA + BC Velocity contours*



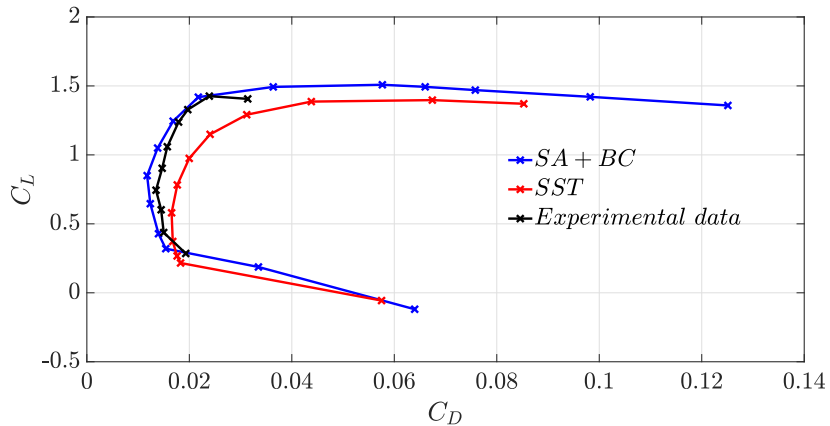
(a) C_L vs α (b) C_D vs α



(a) Streamlines plot around $x/c = 0.65$



(b) C_f on upper and lower surfaces



- ① Problem geometry and setup
- ② Mesh convergence
- ③ Polar

- ④ Law of the Wall
- ⑤ Optimization
- ⑥ Roughness

Law of the Wall

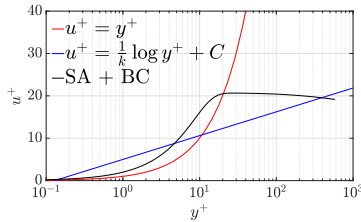
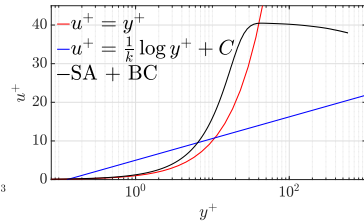
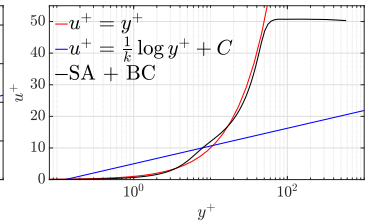
$$y^+ = \frac{yu_\tau}{\nu}$$

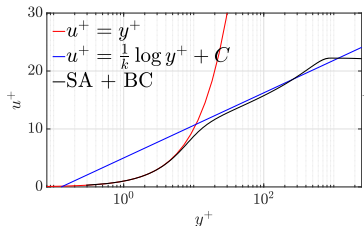
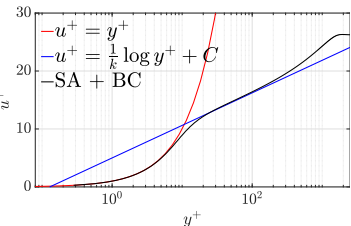
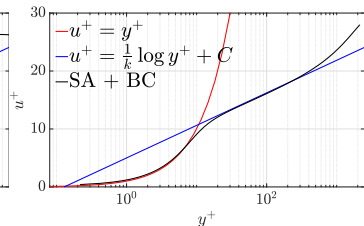
$$u^+ = \frac{u}{u_\tau}$$

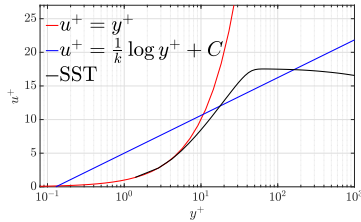
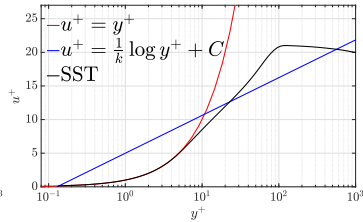
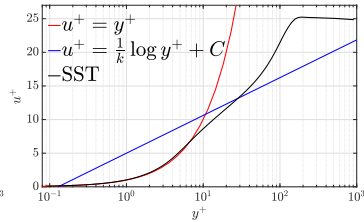
$$u_\tau = \sqrt{\frac{\tau_w}{\rho}}$$

$$\begin{cases} u^+ = y^+ & ; \quad y^+ < 5 \\ u^+ = \frac{1}{k} \ln(y^+) + C & ; \quad y^+ > 30 \end{cases}$$

$$k \sim 0.41 \text{ and } C \sim 5.1$$

(a) $x/C = 0.15, y > 0$ (b) $x/C = 0.365, y > 0$ (c) $x/C = 0.7, y > 0$

(a) $x/C = 0.15, y > 0$ (b) $x/C = 0.365, y > 0$ (c) $x/C = 0.7, y > 0$

(a) $x/C = 0.15, y > 0$ (b) $x/C = 0.365, y > 0$ (c) $x/C = 0.7, y > 0$

- ① Problem geometry and setup
- ② Mesh convergence
- ③ Polar

- ④ Law of the Wall
- ⑤ Optimization
- ⑥ Roughness

Optimization problem

An optimization problem, incorporating a steady state constraint, can be written as

$$\min_{\alpha} J(U(\alpha), X(\alpha))$$

$$\text{subject to } U(\alpha) = G(U(\alpha), X(\alpha)) \quad \text{and} \quad X(\alpha) = M(\alpha)$$

The optimization problem can be subdivided in four main steps:

- geometry parametrization
- RANS simulation
- surface sensitivity calculation $\frac{dJ}{d\alpha}^T$
- mesh deformation

The Lagrangian associated to this optimization problem is defined as

$$L(\alpha, U, X, \Lambda_f, \Lambda_g) = J(U, X) + [G(U, X) - U]^T \Lambda_f + [M(\alpha) - X]^T \Lambda_g$$

If L is differentiated with respect to the design variables α , Λ_f and Λ_g can be set in order to make the flow variables and the mesh independent from the design variables, which leads to a PDE for Λ_f and an algebraic equation for Λ_g . Finally, the sensitivity is obtained as

$$\frac{dL}{d\alpha}^T = \frac{dJ}{d\alpha}^T = \frac{dM(\alpha)}{d\alpha}^T \Lambda_g$$

Models and constraints

The optimization is carried out with the following models:

- incompressible Reynolds-averaged Navier–Stokes (RANS) equations with SA scheme as turbulent model and BC scheme as transition model.
- Jameson-Schmidt-Turkel (JST) scheme as numerical method for the direct and the adjoint simulations.

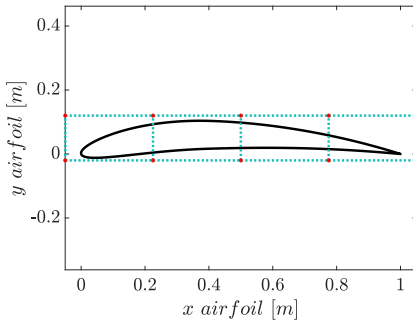
The optimization is performed at two different angles of attack, respectively 2° and 7° , with two constraints imposed on the simulation:

- the airfoil area is set as constant and equal to 0.0617472 m^2 , value obtained with SU2_GEO
- the lift coefficient is bound to be greater than the values calculated with the direct flow simulations

Optimization process

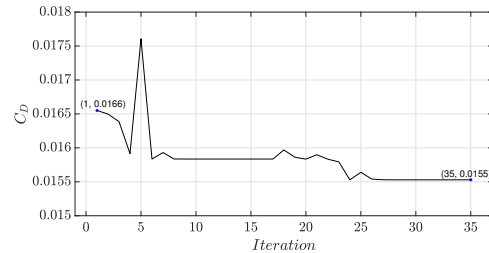
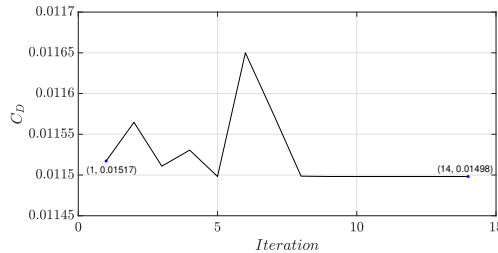
The optimization algorithm in SU2 can be subdivided in two steps:

- **creation of the box** around the airfoil with SU2_DEF; a number of control points equal to 10 is chosen to parameterize the geometry
- **optimization loop** run with shape_optimization.py

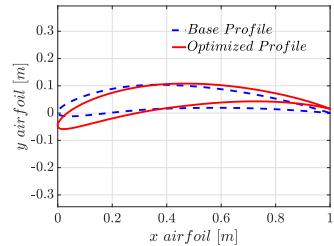
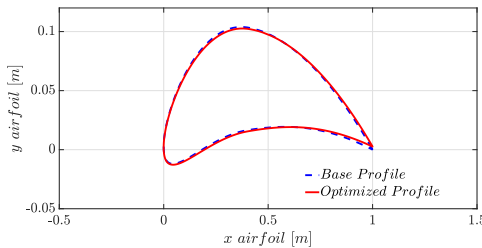


Optimization - Results

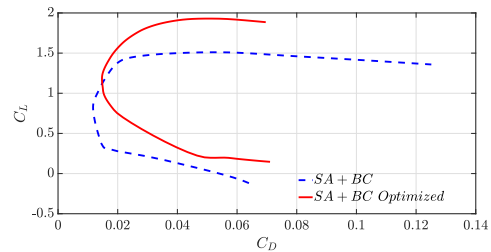
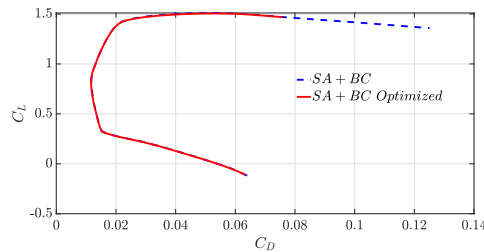
Convergence



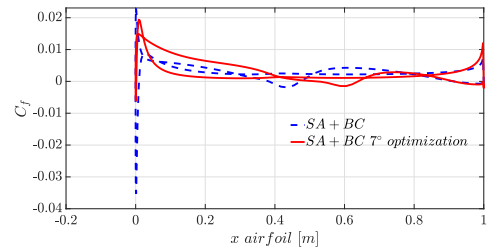
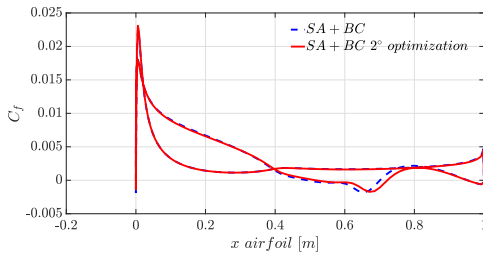
Optimized airfoil shapes



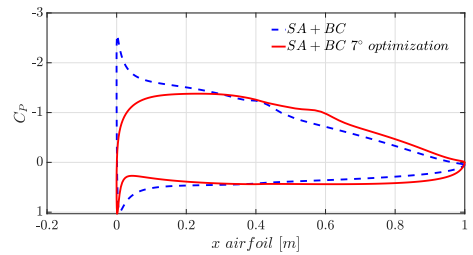
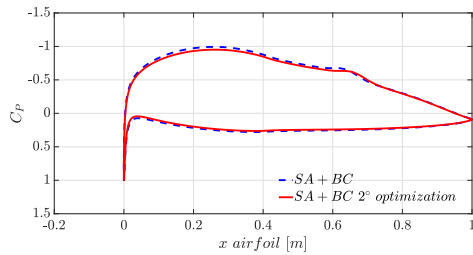
Optimized polars



Optimized skin friction coefficient distributions



Optimized pressure coefficient distributions



- ① Problem geometry and setup
- ② Mesh convergence
- ③ Polar

- ④ Law of the Wall
- ⑤ Optimization
- ⑥ Roughness

Way to characterize roughness? → Equivalent-sand grain approach

Real roughness height → equivalent sand-grain roughness height k_s

Non-dimensional equivalent sand-grain roughness height k_s^+ :

$$k_s^+ = \frac{k_s}{\delta_\nu} = \frac{k_s u_\tau}{\nu}$$

Effect of Roughness

Roughness affects the the velocity profile near the wall

Log-law now function of k_s^+ . Thus:

$u^+ = y^+ \rightarrow$ Viscous sub-layer

$u^+ = \frac{1}{\kappa} \ln\left(\frac{y^+}{k_s^+}\right) + B(k_s^+) \rightarrow$ Log-law

According to the value of k_s^+ , different flow regimes can be identified:

- Smooth regime ($k_s^+ < 5$): $B \sim 5.1$.
- Transitionally-rough regime ($5 < k_s^+ < 70$): B changes with k_s^+
- Fully-rough regime ($k_s^+ > 70$): $B \sim 8.0$

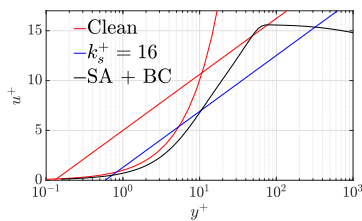
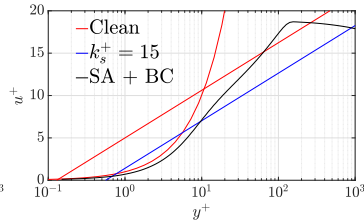
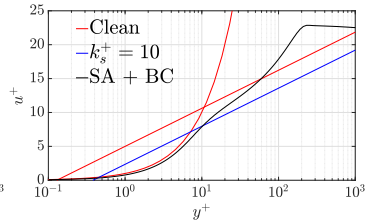
Boeing roughness extension used with SA. Eddy viscosity $\nu_t = \tilde{\nu} f_{v1}$ at the rough wall is set to a finite value. $\tilde{\nu} = 0$ is replaced by:

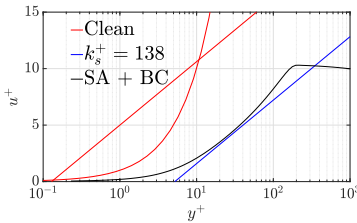
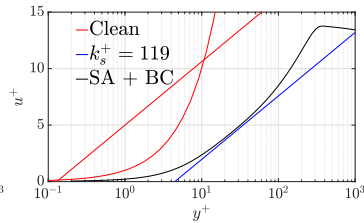
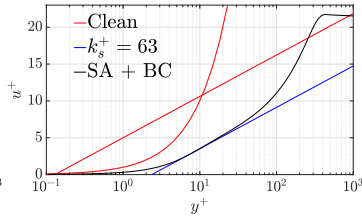
$$\frac{d\tilde{\nu}}{dn} = \frac{\tilde{\nu}}{d}$$

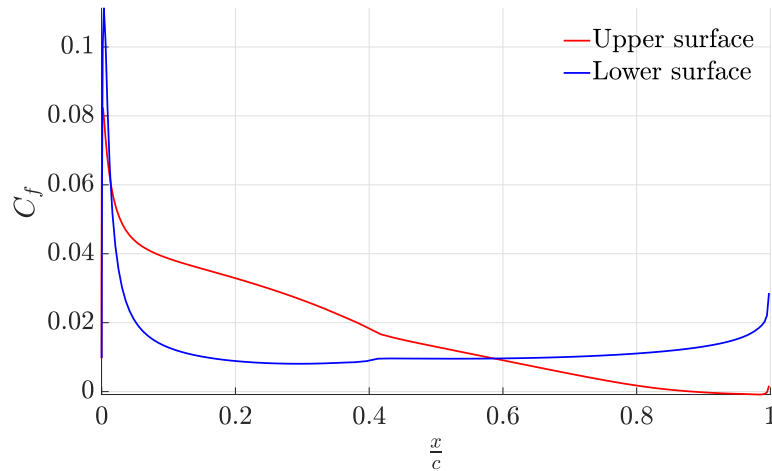
χ in f_{v1} changed to:

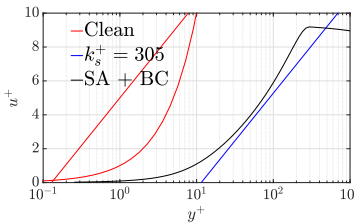
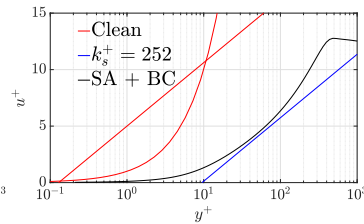
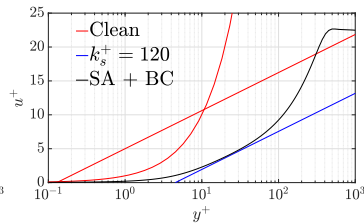
$$\chi = \frac{\tilde{\nu}}{\nu} + 0.5 \frac{k_s}{d}$$

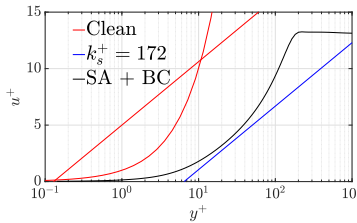
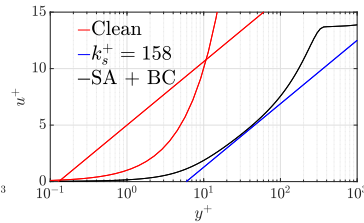
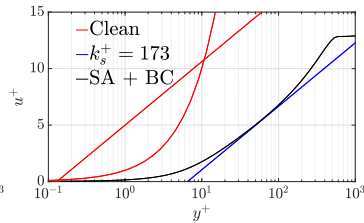
- Evaluate and validate the effects of roughness in the boundary layer

(a) $x/c = 0.15, y > 0$ (b) $x/c = 0.365, y > 0$ (c) $x/c = 0.7, y > 0$

(a) $x/c = 0.15, y > 0$ (b) $x/c = 0.365, y > 0$ (c) $x/c = 0.7, y > 0$

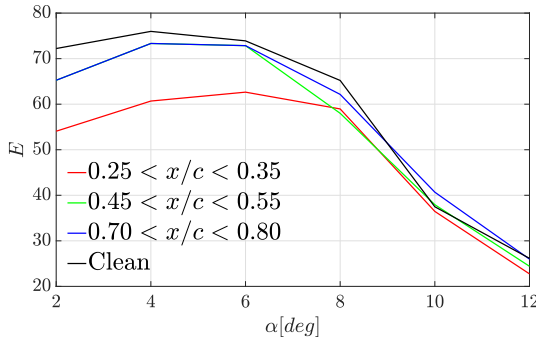
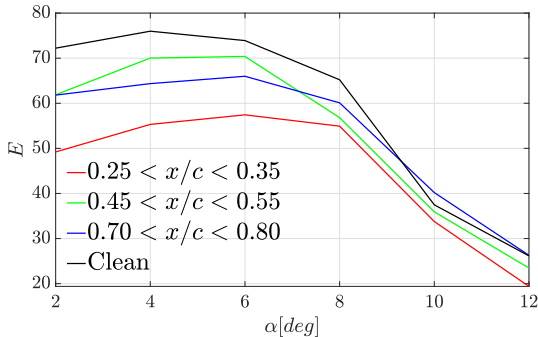
C_f distribution for $\alpha = 2$ and $k_s = 0.012$ 

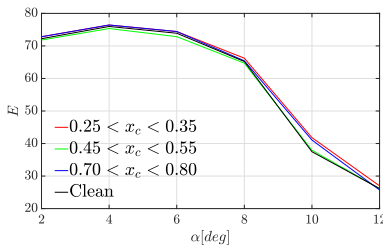
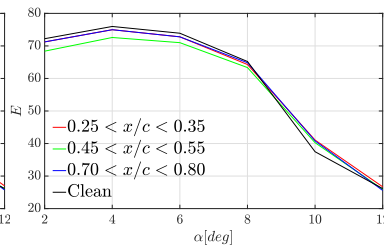
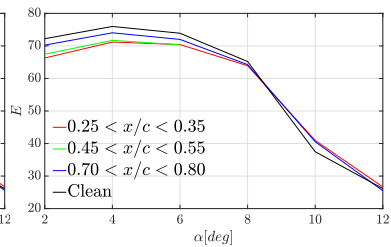
(a) $x/c = 0.15, y > 0$ (b) $x/c = 0.365, y > 0$ (c) $x/c = 0.7, y > 0$

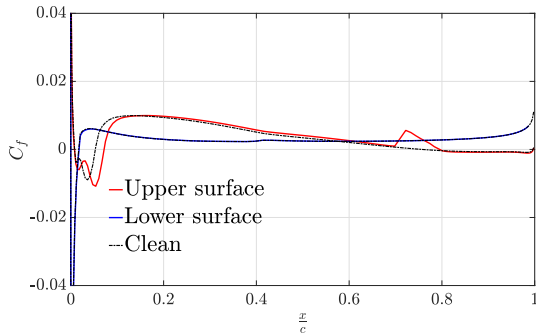
(a) $x/C = 0.15, y < 0$ (b) $x/C = 0.365, y < 0$ (c) $x/C = 0.7, y < 0$

Localised Roughness - Efficiency comparison - Upper surface

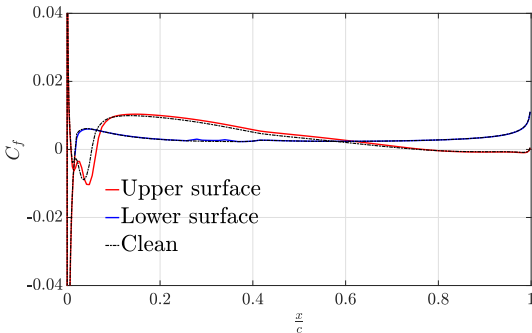
- **Model** and **test** different turbulent trips in different locations
- **Compare** their effects on aerodynamic performance with the clean airfoil's

(a) $k_s = 0.005$ (b) $k_s = 0.01$

(a) $k_s = 0.001$ (b) $k_s = 0.005$ (c) $k_s = 0.01$

Localised Roughness - Comment on C_f at $\alpha = 10^\circ$ 

(a) $k_s = 0.01$. Trip at $0.70 < x/c < 0.85$. Upper surface



(b) $k_s = 0.001$. Trip at $0.25 < x/c < 0.35$. Lower surface